AIP | The Journal of Chemical Physics

Rovibronically selected and resolved two-color laser photoionization and photoelectron study of cobalt carbide cation

Huang Huang, Yih Chung Chang, Zhihong Luo, Xiaoyu Shi, Chow-Shing Lam et al.

Citation: J. Chem. Phys. **138**, 094301 (2013); doi: 10.1063/1.4790707
View online: http://dx.doi.org/10.1063/1.4790707
View Table of Contents: http://jcp.aip.org/resource/1/JCPSA6/v138/i9
Published by the American Institute of Physics.

Additional information on J. Chem. Phys.

Journal Homepage: http://jcp.aip.org/
Journal Information: http://jcp.aip.org/about/about_the_journal
Top downloads: http://jcp.aip.org/features/most_downloaded
Information for Authors: http://jcp.aip.org/authors

ADVERTISEMENT

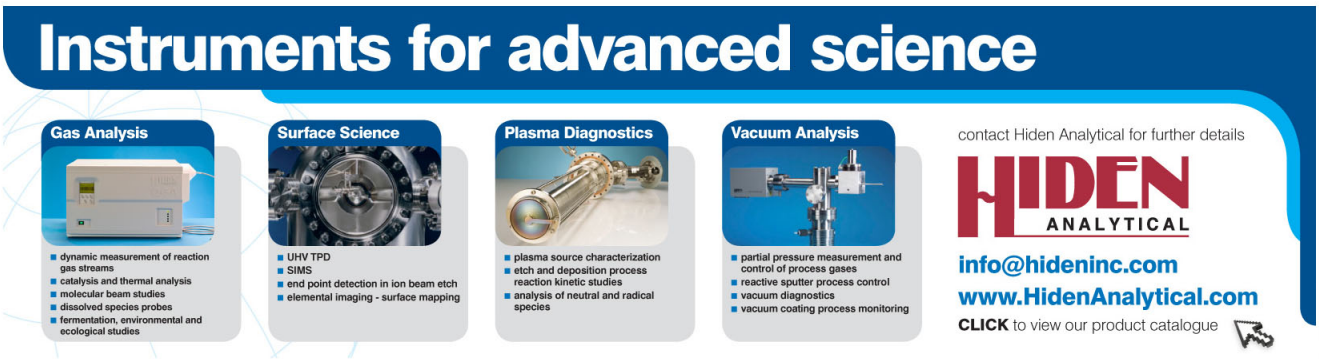

Downloaded 07 Mar 2013 to 18.85.28.26. Redistribution subject to AIP license or copyright; see http://jcp.aip.org/about/rights_and_permissions

Rovibronically selected and resolved two-color laser photoionization and photoelectron study of cobalt carbide cation

Huang Huang,[1] Yih Chung Chang,[1] Zhihong Luo,[1] Xiaoyu Shi,[1] Chow-Shing Lam,[1] Kai-Chung Lau,[2] and C. Y. Ng[1,a)]
[1]*Department of Chemistry, University of California, Davis, California 95616, USA*
[2]*Department of Biology and Chemistry, City University of Hong Kong, Kowloon, Hong Kong*

(Received 7 December 2012; accepted 25 January 2013; published online 1 March 2013)

We have conducted a two-color visible-ultraviolet (VIS-UV) resonance-enhanced laser photoionization efficiency and pulsed field ionization-photoelectron (PFI-PE) study of gaseous cobalt carbide (CoC) near its ionization onset in the total energy range of 61 200–64 510 cm^{-1}. The cold gaseous CoC sample was prepared by a laser ablation supersonically cooled beam source. By exciting CoC molecules thus generated to single N' rotational levels of the intermediate $CoC^*(^2\Sigma^+; v')$ state using a VIS dye laser prior to UV laser photoionization, we have obtained N^+ rotationally resolved PFI-PE spectra for the $CoC^+(X^1\Sigma^+; v^+ = 0$ and 1) ion vibrational bands free from interference by impurity species except Co atoms produced in the ablation source. The rotationally selected and resolved PFI-PE spectra have made possible unambiguous rotational assignments, yielding accurate values for the adiabatic ionization energy of $CoC(X^2\Sigma^+)$, IE(CoC) = 62 384.3 ± 0.6 cm^{-1} (7.73467 ± 0.00007 eV), the vibrational frequency $\omega_e{}^+ = 985.6 \pm 0.6$ cm^{-1}, the anharmonicity constant $\omega_e{}^+\chi_e{}^+ = 6.3 \pm 0.6$ cm^{-1}, the rotational constants ($B_e{}^+ = 0.7196 \pm 0.0005$ cm^{-1}, $\alpha_e{}^+ = 0.0056 \pm 0.0008$ cm^{-1}), and the equilibrium bond length $r_e{}^+ = 1.534$ Å for $CoC^+(X^1\Sigma^+)$. The observation of the $N^+ = 0$ level in the PFI-PE measurement indicates that the CoC^+ ground state is of $^1\Sigma^+$ symmetry. Large $\Delta N^+ = N^+ - N'$ changes up to 6 are observed for the photoionization transitions $CoC^+(X^1\Sigma^+; v^+ = 0–2; N^+) \leftarrow CoC^*(^2\Sigma^+; v'; N' = 6, 7, 8,$ and 9). The highly precise energetic and spectroscopic data obtained in the present study have served as a benchmark for testing theoretical predictions based on state-of-the-art *ab initio* quantum calculations at the CCSDTQ/CBS level of theory as presented in the companion article. © *2013 American Institute of Physics*. [http://dx.doi.org/10.1063/1.4790707]

I. INTRODUCTION

Because of the high nuclear stability, the iron group transition metal elements (M = Fe, Ni, and Co) are known to exist in abundance in the universe.[1–3] The carbides of the iron group transition metals (MCs) are also expected to exist in stellar objects and interstellar media, especially in the carbon rich envelope of stars.[3] Thus, the spectroscopic and energetic studies of MC molecules are of relevance to astrophysics.[1,2] Transition metal carbides and their clusters are also recognized to be technologically important compounds partly due to their catalytic activities.[2,4,5] Many previous studies on the iron group transition metal carbides have been motivated to understand their electronic structures and bonding properties,[2,4–9] which are believed to be responsible for their catalytic function. Being the simplest transition metal carbides, the MC molecules and their cations (MC^+s) represent an ideal system for detailed experimental[10,11] and theoretical[12–16] investigations to gain fundamental understanding on the bonding characters of the transition metal carbides and their clusters.

The studies of transition metal-containing compounds in the gas phase are challenging both experimentally and theoretically.[10–16] The major challenge in experimental studies is the difficulty in generating transition metal-containing molecules in the gas phase with a sufficiently high intensity and purity. In addition, the existence of low-lying excited electronic states with different multiplicities for the MC/MC^+ species are expected to give rise to complex spectroscopic transition structures in a spectroscopy study, making their assignment difficult. Accurate theoretical predictions on the energetic and structural properties of the MC species have also been hindered by the significant relativistic effects and the proper description of the multi-reference characters of the molecular wavefunctions.[12–14] In view of these experimental and theoretical difficulties, highly accurate structural and energetic data for most of the transition metal carbides and their cations remain to be determined.

In an effort to establish a highly precise energetic database for simple transition metal oxides and carbides and their cations, we have initiated a research program to perform high-resolution photoionization efficiency (PIE) and pulsed field ionization-photoelectron (PFI-PE) measurements of transition metal-containing species.[10,11] The ionization energies (IEs) of many of the transition metal carbides and oxides are in the energy range of 6.5–10.0 eV. When a stable intermediate neutral state for these species is known, they are ideal candidates for two-color visible-ultraviolet (VIS-UV) laser

a)Electronic mail: cyng@ucdavis.edu.

 © 2013 American Institute of Physics

Downloaded 07 Mar 2013 to 18.85.28.26. Redistribution subject to AIP license or copyright; see http://jcp.aip.org/about/rights_and_permissions

PIE and PFI-PE studies,[10,11] from which highly precise IE and spectroscopic constants can be determined by rotationally selected and resolved photoelectron measurements. Recently, we have successfully investigated the FeC^+ and NiC^+ cations by means of two-color VIS-UV resonance-enhanced PIE and PFI-PE measurements.[10,11] By first exciting FeC (NiC) to a single rovibronic level of an intermediate neutral state FeC* (NiC*) by a VIS dye laser prior to photoionization by a UV dye laser, we have been able to select the FeC (or NiC) molecules from a mixture of impurity compounds produced in the laser ablation source for PIE and PFI-PE studies. The PFI-PE spectra for the vibrational bands of FeC^+ (NiC^+) thus obtained are completely rotationally resolved and free from spectral interference from impurity compounds except Fe (Ni) atoms produced in the laser ablation source. The highly precise energetic data, such as IEs, and the difference between the 0 K bond dissociation energy (D_0) for MC^+ and that for MC for the FeC/FeC^+ and NiC/NiC^+ systems thus obtained have been used as a benchmark for state-of-the-art *ab initio* quantum chemical calculations, aiming to help develop more reliable quantum computation procedures for accurate structural and energetic predictions of transition metal-containing compounds. While the experimental IE(FeC) [IE(NiC)] and $D_0(Fe^+\text{-}C) - D_0(Fe\text{-}C)$ [$D_0(Ni^+\text{-}C) - D_0(Ni\text{-}C)$] values were found to have significant deviations from the theoretical predictions obtained by the multi-reference variation method at the C-MRCI+Q level of theory[10,11,14–16] and density functional theory[13] (DFT) calculations, the experimental energetic values are in surprisingly good agreement with the calculated results based on the CCSDTQ/CBS approach,[15,16] which involves the approximation to the complete basis set (CBS) limit at the coupled cluster level up to quadruple excitations.

Many experimental[3,6–9] and theoretical[12–14] studies on neutral CoC had been reported in the literature. The early electron spin resonance study of CoC in Ar matrices reveals that the ground electronic state of CoC is of $^2\Sigma$ symmetry.[6] A high-resolution laser induced fluorescence study of CoC has provided spectroscopic constants for the $X^2\Sigma^+$ ground state and three low-lying excited electronic states ($^2\Delta_{5/2}$, $^2\Pi_{3/2}$, and $^2\Pi_{1/2}$) of CoC.[8] Subsequent spectroscopic studies of CoC have identified a long vibrational progression $CoC(F^2\Sigma^+; v' = 0\text{–}13) \leftarrow CoC(X^2\Sigma^+; v'' = 0)$ in the energy range of 13 500 to 22 000 cm^{-1}.[7,9] The most accurate values for the rotational constant (B'') and bond length of the CoC ($X^2\Sigma^+$; $v'' = 0$) ground state were determined by the sub-millimeter-wave study of Brewster and Ziury.[3] Despite all these spectroscopic studies on neutral CoC, no spectroscopic investigations on CoC^+ have yet been reported. On the theoretical side, Gutsev *et al.* have performed a theoretical study on 3*d*-transition metal carbides and oxides and their anions and cations by means of DFT calculations,[13] predicting a value of 7.99 eV for the IE(CoC) along with spectroscopic constants for CoC^+. Recently, high-level multi-reference *ab initio* quantum calculations on the ground and low-lying excited states of CoC have been reported by Borin *et al.*[12] and Tzeli and Mavridis[14] The MRCI theoretical calculation predicts that CoC has two lowest electronic states, $^2\Sigma^+$ and $^2\Delta$, with the respective main configurations of $\ldots 7\sigma^2\ 8\sigma^2\ 3\pi^4\ 1\delta^4\ 9\sigma^1$ and $\ldots 7\sigma^2\ 8\sigma^2\ 3\pi^4\ 1\delta^3\ 9\sigma^2$, and that the first excited $CoC(^2\Delta)$ state is located only ≈30 meV higher than the $CoC(^2\Sigma^+)$ ground state.[14,17] This prediction is consistent with the results of the laser induced fluorescence study.[8] Thus, photoionization of $CoC(X^2\Sigma^+)$ should involve the ejection of the unpaired electron residing in the highest occupied 9σ molecular orbital, resulting in the CoC^+ ground state with $^1\Sigma^+$ symmetry. However, when spin-orbit interaction is included, the most recent calculations predict that $CoC(^2\Delta_{5/2})$ becomes the ground state, and is ≈30 meV lower than the $CoC(^2\Sigma^+)$.[14,17] Thus, the IE values to form $CoC^+(X^1\Sigma^+)$ from the $CoC(^2\Delta)$ and $CoC(X^2\Sigma^+)$ states are only separated by ≈30 meV. For a rigorous experimental IE measurement, it is desirable to distinguish the actual photoionization transition.

This article presents the first spectroscopic study on CoC^+ by means of the two-color VIS-UV resonance-enhanced PIE and PFI-PE techniques.[10,11] In addition to the results of previous studies on the FeC/FeC^+ and NiC/NiC^+ systems, the present high-resolution PFI-PE study on the CoC/CoC^+ system has served to provide additional tests for the *ab initio* CCSDTQ/CBS computation procedures for energetic and structural predictions of transition metal-containing compounds. The rotationally selected and resolved PFI-PE spectra for CoC^+ have also allowed the symmetry determination of the CoC^+ ground state. Highly accurate values for the IE(CoC), rotational and vibrational constants for CoC^+, and $D_0(Co^+\text{-}C) - D_0(Co\text{-}C)$ obtained here are compared to the CCSDTQ/CBS predictions in the companion[17] article.

II. EXPERIMENT

The experimental apparatus and procedures used are essentially the same as those employed in the studies on FeC/FeC^+ and NiC/NiC^+ systems and have been described in detail previously.[10,11] Briefly, the apparatus consists of a Smalley-type[18] laser ablation supersonic beam source for the generation of cold CoC molecules, two Nd:YAG laser pumped dye lasers for two-color resonance-enhanced photoionization measurements, a time-of-flight (TOF) mass spectrometer for photoion detection, and a TOF spectrometer for PFI-PE detection. The two dye lasers used in this experiment are the Lambda Physik FL 3002 [VIS output = ω_1, optical bandwidth = 0.2 cm^{-1} (full-width at half-maximum, FWHM)] and FL 2002 [UV output = ω_2, optical bandwidth = 0.4 cm^{-1} (FWHM)] dye lasers, which were pumped by the same Nd:YAG laser (Spectra-Physics, Quanta-Ray Pro 230; repetition rate = 30 Hz).

Gaseous CoC molecules were produced by reacting Co atoms with CH_4 (10% CH_4 seeded in He as the carrier gas). The Co atoms were generated by laser ablation on a rotating and translating Co rod (American Element, 99% purity) by using the second harmonic (532 nm) output of a Nd:YAG laser (Continuum, Surelite-1-30) operating at 30 Hz with a pulse energy of ≈2 mJ. The gaseous CoC sample thus formed was cooled by supersonic expansion and skimmed by a circular skimmer (diameter = 1 mm) in the beam source chamber prior to entering the photoionization/photoexcitation

Downloaded 07 Mar 2013 to 18.85.28.26. Redistribution subject to AIP license or copyright; see http://jcp.aip.org/about/rights_and_permissions

(PI/PEX) region in the photoionization chamber. A pair of deflection plates was installed between the skimmer and the PI/PEX region and was biased at a dc field of ≈150 V/cm to prevent the charged and metastable Rydberg species produced in the laser ablation process from entering the PI/PEX region. This arrangement was found to be effective in reducing the background noise in PFI-PE measurements.

Compared to the FeC/FeC$^+$ and NiC/NiC$^+$ studies,[10,11] the observed CoC$^+$ intensity was found to be significantly lower than those for FeC$^+$ and NiC$^+$ under the same operational conditions of the laser ablation source. We have improved the observed CoC$^+$ signal by water cooling the laser ablation source, such that higher laser pulse energies (≈2 mJ) can be used effectively for the ablation of the Co rod to produce a higher CoC intensity. Similar to the previous FeC/FeC$^+$ and NiC/NiC$^+$ studies, this CoC/CoC$^+$ experiment was concerned with three types of measurements, including the excitation spectra of the selected intermediate CoC* state and the two-color VIS-UV resonance-enhanced PIE and PFI-PE spectra for CoC$^+$.

The selection of an appropriate excited intermediate CoC* state is essential for the success of the two-color resonance-enhanced PIE and PFI-PE measurements. It is desirable for the selected CoC* state to have a vibrational band with high excitation intensity, long lifetime, and well-resolved rotational transitions. We have surveyed the excitation spectra for the vibronic transition bands appearing in the energy range of 18 000–21 000 cm^{-1}, from which the vibronic band at 20 408.0 cm^{-1} [20.4] was chosen as the intermediate CoC* state[7–9] for two-color VIS-UV laser resonance-enhanced PIE and PFI-PE measurements because of its high intensity and long lifetime (0.12 μs).[9] Figure 1 depicts the rovibronically resolved excitation spectrum (upper spectrum) of the intermediate [20.4] vibronic band obtained by setting the UV ω_2 frequency at 47 620 cm^{-1} and scanning the VIS ω_1 frequency in the energy range of 20 340–20 422 cm^{-1}. Based on the previous study, this [20.4] vibronic band was assigned to arise from the excitation transitions CoC*($^2\Sigma^+$; v'; N') ← CoC($X^2\Sigma^+$; v'' = 0; N''). However, the assignment of the v' vibration quantum number for this intermediate vibronic band was not made.

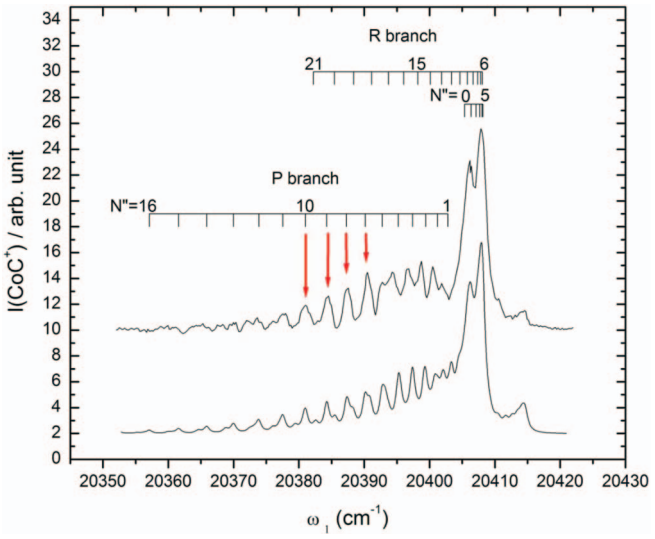

FIG. 1. The rotational-resolved excitation spectrum (upper curve) for the formation of the intermediate CoC*($^2\Sigma^+$; v'; N') rovibronic states from the CoC($X^2\Sigma^+$; v'' = 0; N'') ground state. This spectrum was recorded by means of two-color VIS-UV laser resonance-enhanced photoionization scheme, in which the UV ω_2 laser was fixed at 47 620 cm^{-1} and the VIS ω_1 was scanned in the energy range of 20 300–20 420 cm^{-1}. The simulated spectrum (lower curve) was obtained by using a Gaussian instrumental line profile (FWHM = 1.0 cm^{-1}) and a Boltzmann rotational temperature of 35 K for the CoC molecular beam.

During the two-color VIS-UV resonance-enhanced PIE and PFI-PE measurements, the VIS ω_1 energy can be fixed at the band head at 20 408.5 cm^{-1} of the excitation spectrum shown in Fig. 1. Since the band head gives the highest excitation intensity to the intermediate CoC*($^2\Sigma^+$; v') state, this excitation results in the highest CoC$^+$ signal. However, in this case several N' rotational levels of the CoC*($^2\Sigma^+$; v') state are populated; and thus all these N' rotational levels are expected to contribute to the observed PIE and PFI-PE intensities. When the VIS ω_1 energy is fixed at the transition energy of a well-resolved rotational transition as marked by the downward pointing red arrows in Fig. 1, a single N' rotational level of the CoC*($^2\Sigma^+$; v') state is selected for photoionization by the UV ω_2 laser. In the VIS-UV PIE and PFI-PE measurements presented here, the UV ω_2 frequency was tuned in the range of 41 656–44 122 cm^{-1} in order to cover the photoionization thresholds for the formation of CoC$^+$($X^1\Sigma^+$; v^+ = 0, 1, and 2) from the intermediate CoC*($^2\Sigma^+$; v') state.

The ions formed by photoionization were extracted toward the TOF mass spectrometer for detection by the ion MCP detector by applying a dc electric field of 10 V/cm in the PI/PEX region. For PFI-PE measurements, we found that it is necessary to keep the PI/PEX region field free during the laser excitation in order to minimize the destruction of high-n Rydberg species.[19] Hence, the pulsing scheme for PFI-PE measurements adopted in the present study is slightly different from that used in the previous FeC/FeC$^+$ and NiC/NiC$^+$ experiments.[10,11] Here, an electric field of 0.1 V/cm for the dispersion of prompt background electrons was applied to the PI/PEX region at a delay of 150 ns with respect to the application of the UV ω_2 laser pulse. The electric field pulse of 0.5 V/cm for PFI and the extraction of PFI-PEs toward the electron MCP detector were turned on at a delay of 1.5 μs with respect to the UV ω_2 laser pulse. The energies of both dye lasers were calibrated by using a Coherent WaveMaster to a precision of ±0.04 cm^{-1}.

The ion or electron signal from the MCP detector was amplified by a fast preamplifier (LeCroy research system, 612AM) before being fed into a gated boxcar integrator (Stanford Research system, SR250) for data integration. The analog signal thus obtained was converted to digital data by using an analog to digital converter (Stanford research system, SR245) for data processing by a personal computer. At each setting of the laser energies, the data obtained represent the average of 30 laser shots and the photoion and PFI-PE intensities have been normalized by the UV ω_2 laser power. All PIE and PFI-PE spectra presented in this study are the average of at least four independent, reproducible scans.

Downloaded 07 Mar 2013 to 18.85.28.26. Redistribution subject to AIP license or copyright; see http://jcp.aip.org/about/rights_and_permissions

III. RESULTS AND DISCUSSION

For the CoC($X^2\Sigma^+$) ground and the CoC*($^2\Sigma^+$) intermediate states, their respective projected electronic orbital angular momenta along the internuclear axes Λ'' and Λ' are zero. Since there is no magnetic field to align the spin angular momentum to the internuclear axis, the angular momentum coupling for the ground (intermediate) state is expected to obey the Hund's case (b) scheme. By ignoring the spin-rotation coupling, the rotational energy F(N'') [F(N')] can be expressed as: $F(N'') = B_v''(N'')(N''+1)$ [$F(N') = B_v'(N')(N'+1)$], where N'' (N') is the rotational quantum number, B_v'' (B_v') is the rotational constant of the CoC($X^2\Sigma^+$; v'') [CoC*($^2\Sigma^+$; v')] state. Using these equations along with the standard formula: $G(v) = \omega_e(v+1/2) - \omega_e\chi_e(v+1/2)^2$ for the vibrational energy, the energies for the rovibronic transitions, CoC*($^2\Sigma^+$; v'; N') ← CoC($X^2\Sigma^+$; v''; N''), can be identified by simulation based on the equation

$$v = v_{v'v''} + B_{v'}(N')(N'+1) - B_{v''}(N'')(N''+1). \quad (1)$$

Here, $\nu_{v'v''} = \nu_{v'0} = \Delta T_{e'e''} + G(v') - G(v''=0)$ is the origin for the v' vibrational band, $\Delta T_{e'e''}$ is the energy separation between the potential minimum of the CoC*($^2\Sigma^+$) intermediate state and that of the CoC($X^2\Sigma^+$) ground state, and $G(v')$ and $G(v'')$ are the vibrational energies for the intermediate and ground states, respectively. For simplicity, the band origin for the formation of the neutral CoC*($^2\Sigma^+$; v') and the ion CoC^+($X^1\Sigma^+$; v^+) states from the neutral CoC($X^2\Sigma^+$; $v''=0$) ground state will be designated as $\nu_{v'}$ and ν_{v+}, respectively.

In order to assign the rotational transitions resolved in the excitation spectrum (upper spectrum) of Fig. 1, we have undertaken a simulation of this spectrum. The simulation assumes a Gaussian instrumental profile (FWHM = 1.0 cm^{-1}) and a Boltzmann distribution of N'' rotational levels for CoC($X\ ^2\Sigma^+$; $v''=0$) governed by a rotational temperature. The highly precise rotational constant $B'' = 0.6937502\ cm^{-1}$ for the CoC($X^2\Sigma^+$) ground state determined previously by Barnes *et al.*[8] was adopted here directly in the simulation exercise. The rotational transition energies are calculated by using the standard formula of Eq. (1). The best simulated spectrum (shown as the lower spectrum of Fig. 1) yields the band origin $\nu_{v'} = 20404.2\ cm^{-1}$ and the rotational constant $B' = 0.595\ cm^{-1}$. This B' value is significantly smaller than the B'' value; but is consistent with the rotational constants for intermediate vibrational bands of CoC determined in this energy region.[7–9] As an example, the rotational constant for the $F^2\Sigma^+$ state was determined to be $0.5530\ cm^{-1}$. According to the report of Guo *et al.*,[9] the [20.4] intermediate state used here is not a $F^2\Sigma^+(v')$ state, but is another electronic state of $^2\Sigma^+$ symmetry with a high v' value. The simulation also provides a rotational temperature of 35 K for CoC($X\ ^2\Sigma^+$; $v''=0$). The identification of the P(N'') and R(N'') transitions based on the best simulated spectrum is marked on top of the excitation spectrum of Fig. 1. The observation of the P and R-branches, but not the Q-branch is consistent with the $\Omega' = 0 \leftarrow \Omega'' = 0$ transition between the ground and the intermediate states involved in this case. The comparison of the excitation and simulated spectra in Fig. 1 suggested that the spectral region covering the rotational lines, P(N''), N'' = 1–6, is likely contaminated by other weak transitions. In order to obtain cleanly rotationally resolved PFI-PE spectra for the $v^+ = 0$, 1, and 2 vibrational bands, it is necessary to prepare the intermediate CoC* state in a single rotational level with high purity. The P(N'') rotational transitions, P(7), P(8), P(9), and P(10) (marked by downward pointing red arrows), are the most well-resolved transitions in the excitation spectrum of the [20.4] vibronic band. For this reason, we have selected these rotational transitions for the preparation of the respective rovibronic states CoC*($^2\Sigma^+$; v'; $N' = 6$, 7, 8, and 9) by VIS ω_1 excitation.

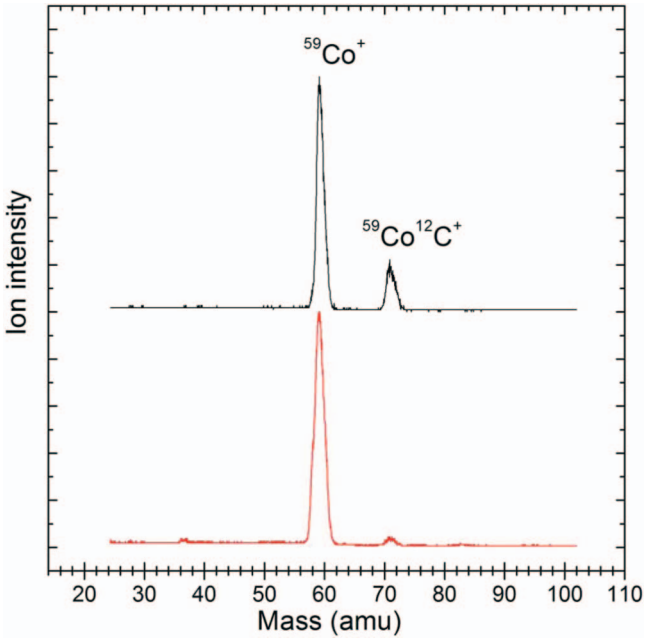

FIG. 2. The upper spectrum is the TOF mass spectrum for Co^+ and CoC^+ observed by setting the VIS ω_1 energy at the band head (20 408.5 cm^{-1}) of the excitation spectrum shown in Fig. 1 and the UV ω_2 energy at 47 620 cm^{-1}. The lower TOF mass spectrum was obtained when the VIS ω_1 laser was blocked off, i.e., only the UV ω_2 laser was employed for the photoionization sampling of the Co and CoC beam.

The TOF mass spectra obtained by means of the two-color VIS-UV laser resonance-enhanced photoionization scheme by setting the VIS $\omega_1 = 20\,408.5\ cm^{-1}$ and UV $\omega_2 = 47\,620\ cm^{-1}$ are shown as the upper spectrum in Fig. 2. The observed ion peaks at 59 and 71 amu are identified as Co^+ and CoC^+, respectively. The lower spectrum was recorded when the VIS ω_1 laser beam was blocked off, i.e., only the UV ω_2 laser beam was employed to intersect the molecule beam. As shown in Fig. 2, the intensity of the Co^+ ion peak observed in the lower mass spectrum remains the same as that in the upper mass spectrum. However, the intensity of the CoC^+ ion peak appeared in the lower mass spectrum was found to fall significantly to ≤10% of that observed in the upper mass spectrum. This comparison clearly shows that nearly all Co^+ ions are produced by single-color UV two-photon or multi-photon ionization, whereas more than 90% of the observed CoC^+ intensity is formed by two-color VIS-UV laser resonance-enhanced photoionization.

Downloaded 07 Mar 2013 to 18.85.28.26. Redistribution subject to AIP license or copyright; see http://jcp.aip.org/about/rights_and_permissions

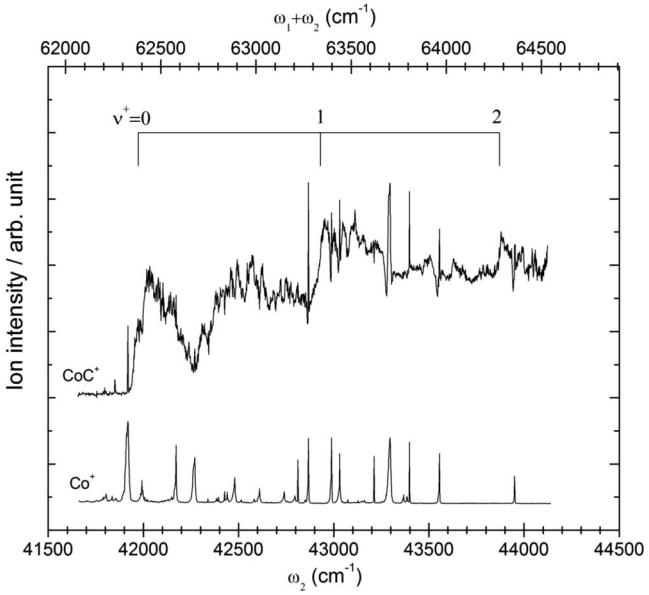

FIG. 3. The PIE spectrum (upper curve) for the formation of $CoC^+(X^1\Sigma^+; v^+ = 0–2)$ recorded by using the two-color VIS-UV laser resonance-enhanced photoionization scheme, in which the VIS ω_1 energy was fixed at $\omega_1 = 20\,408.5\ cm^{-1}$, while the UV ω_2 energy was scanned in the energy range of 41 657–44 120 cm^{-1}. The lower spectrum represents the one-color two-photon UV-UV resonance-enhanced photoion spectrum of Co atom observed in the same UV range. The bottom energy scale represents the UV ω_2 energy, and the top energy scale represents the sum of the VIS and UV (or $\omega_1 + \omega_2$) energy. Three step onsets at 62 381 cm^{-1}, 63 363 cm^{-1}, and 64 301 cm^{-1} (marked on top of the PIE spectrum) are assigned as the ionization thresholds for the formation of $CoC^+(X^1\Sigma^+)$ in the $v^+ = 0$, 1, and 2 states, respectively.

We have obtained the two-color VIS-UV laser resonance-enhanced PIE spectrum of $CoC^+(X^1\Sigma^+)$ near its ionization threshold in the total VIS + UV (or $\omega_1 + \omega_2$) energy range of 62 066–64 529 cm^{-1}, which is shown as the upper spectrum in Fig. 3. This PIE spectrum was obtained by measuring the CoC^+ ion intensity with the VIS ω_1 fixed at 20 408.5 cm^{-1}, while scanning the UV ω_2 output in the range of 41 650–44 120 cm^{-1}. For all the PIE and PFI-PE spectra presented here, the bottom scale of the spectra represents the UV ω_2 energy, while the top scale represents the total VIS and UV ($\omega_1 + \omega_2$) energy. Since setting ω_1 at 20 408.5 cm^{-1} corresponds to the strongest peak of the excitation spectrum shown in Fig. 1, the simulation shows that at this excitation energy the R(N''), $N'' = 3–7$, transitions can contribute, i.e., the $N' = 4–8$ levels of the intermediate $CoC^*(^2\Sigma^+; v')$ state are populated.

The photoion spectrum for Co^+ was also measured (depicted as the lower spectrum of Fig. 3) for comparison with the two-color VIS-UV PIE spectrum of CoC^+. The photoion spectrum for Co^+ was found to exhibit sharp resonances, indicating that they are produced predominantly by resonance enhanced two-photon UV-UV photoionization of Co atoms. As shown in Fig. 3, these sharp atomic resonances observed in the Co^+ spectrum coincide with the sharp structures appearing in the PIE spectrum of CoC^+. This comparison clearly shows that the detection of CoC^+ was interfered by the formation of Co^+ near the atomic resonances. A similar observation was reported previously in the two-color VIS-UV PIE and PFI-PE study of the NiC/NiC^+ system.[11] The overwhelmingly high intensities of Co^+ ions produced near the Co atomic resonances by two-photon UV-UV photoionization were found to have the effect of saturating the ion MCP detector and shifting the ion detection baseline as well as the arrival time of CoC^+ in the TOF measurements, resulting in the reduction of the CoC^+ intensity measured by the gated Boxcar detection. Thus, we can conclude that the sharp structures appearing in the PIE spectrum for CoC^+ near the vicinity of the atomic Co resonance lines are artifacts. The fact that the intensity of CoC^+ was much weaker than that of Co^+, the modulation of the PIE spectrum for CoC^+ by the Co^+ detection near the atomic resonances could not be eliminated by reducing the bias voltage applied to the MCP detector without sacrificing the signal-to-noise ratio for CoC^+ measurements.

Although the two-color VIS-UV PIE spectrum for CoC^+ displays significant modulation structures arisen from the interference by the Co^+ detection near the Co atomic resonances as described above, a sharp PIE step at the total $\omega_1 + \omega_2$ energy of 62 381 cm^{-1} is clearly evident. This position of the PIE step can be assigned as the adiabatic IE for the formation of $CoC^+(X^1\Sigma^+; v^+ = 0)$ from $CoC(X\ ^2\Sigma^+; v'' = 0)$ as the CoC^+ signal at total energies below this step is found to be at the noise level. Another two PIE steps are observed at 63 363 and 64 301 cm^{-1}, which can be assigned as the onsets associated with the formation of $CoC^+(X^1\Sigma^+; v^+ = 1$ and 2) from $CoC(X\ ^2\Sigma^+; v'' = 0)$, respectively. These assignments give a rough estimate of about 1000 cm^{-1} for the vibrational spacing of the $CoC^+(X^1\Sigma^+)$ ground state. The measurement of the two-color PIE spectrum for $CoC^+(X^1\Sigma^+; v^+ = 0$, 1, and 2) is an important step for the successful measurement of the two-color VIS-UV PFI-PE spectrum for CoC^+ as the location of the vibrational steps can focus our attention for searching the PFI-PE signal in narrow energy regions near the ionization thresholds for $CoC^+(X^1\Sigma^+; v^+ = 0$, 1, and 2).

Figures 4(a)–4(c) depict the rotationally selected and resolved PFI-PE spectra (lower spectra) for the formation of $CoC^+(X^1\Sigma^+; v^+ = 0; N^+)$ by photoionization from the respective single rotational states, $N' = 6–9$, by setting the VIS ω_1 energy at the respective rotational transitions P(7), P(8), P(9), and P(10) lines of the excitation spectrum shown in Fig. 1. Six dominant peaks (marked with asterisks) observed in these PFI-PE spectra are found to coincide with the Co atomic resonances. The fact that the intensities of these background peaks were found to depend solely on the UV ω_2 laser pulse energy indicates that these background electron peaks originate from two-photon resonance-enhanced UV-UV photoionization of Co atoms. Due to the overwhelmingly high intensities of background electrons produced at the Co resonance lines, the delay PFI scheme could not discriminate all the background electrons from the PFI-PE detection. Fortunately, in this case, the rotational PFI-PE peaks for CoC^+ appearing between these strong background electron peaks are cleanly resolved, such that an unambiguous rotational analysis and assignment of the PFI-PE spectra for $CoC^+(X^1\Sigma^+; v^+ = 0; N^+)$ can be made. The upper spectra shown in Figs. 4(a)–4(d) are the corresponding simulated spectra obtained by

Downloaded 07 Mar 2013 to 18.85.28.26. Redistribution subject to AIP license or copyright; see http://jcp.aip.org/about/rights_and_permissions

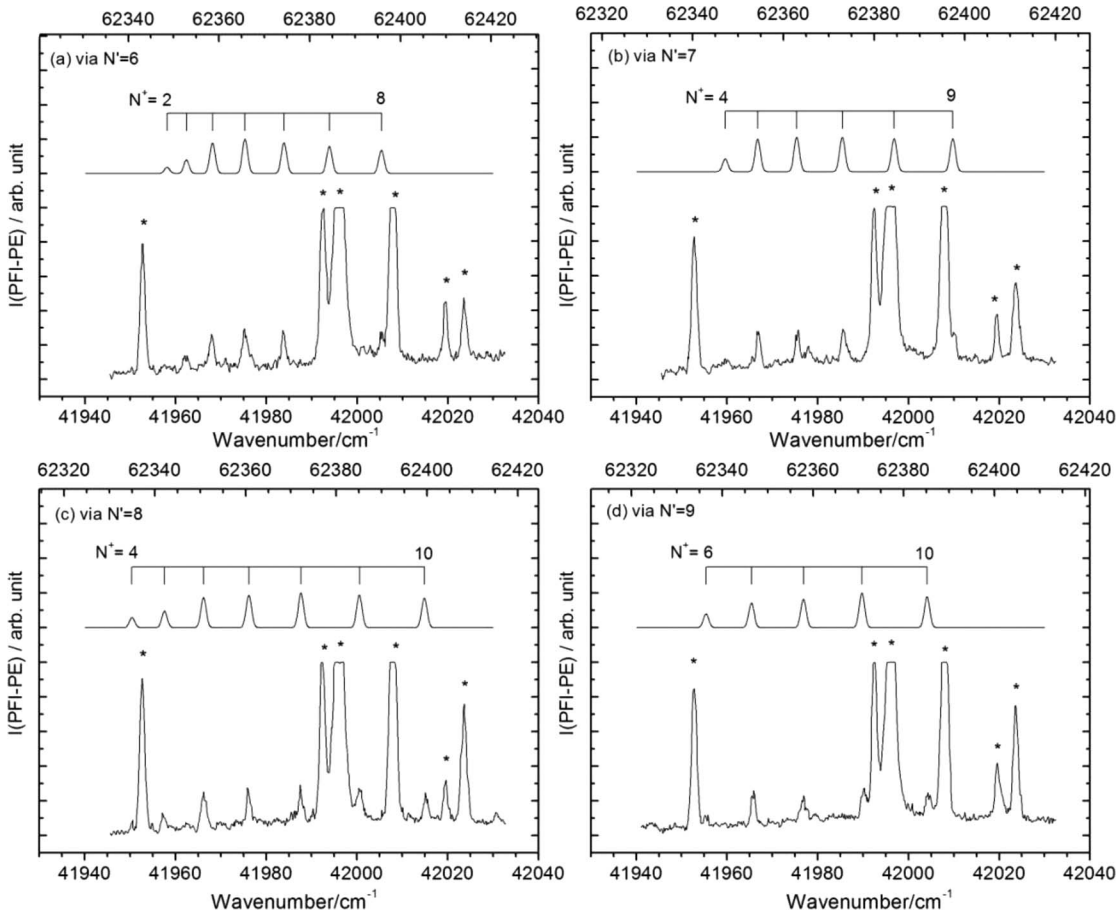

FIG. 4. Rotationally selected and resolved PFI-PE spectra (lower spectra) in the total $\omega_1 + \omega_2$ energy region of 62 330–62 420 cm^{-1} (top energy scale) for the formation of $CoC^+(X^1\Sigma^+; v^+ = 0; N^+)$ from the rotational levels, (a) $N' = 6$, (b) $N' = 7$, (c) $N' = 8$, and (d) $N' = 9$, of the intermediate $CoC^*(^2\Sigma^+; v')$ state. The corresponding UV ω_2 energies are in the range of 41 945–42 032 cm^{-1} (bottom energy scale). These N' levels were prepared by setting the VIS ω_1 energy at the respective P(7), P(8), P(9), and P(10) transition positions as marked in the excitation spectrum of Fig. 1. The individual simulated spectra obtained by using a Gaussian instrumental line profile (FWHM = 1.5 cm^{-1}) for the PFI-PE energy resolution profile are shown as the upper curves in (a)–(d). The peaks marked by asterisks are background electron peaks originated from electrons produced by one-color UV-UV resonance-enhanced photoionization of Co atoms.

assuming a Gaussian instrumental profile (FWHM = 1.5 cm^{-1}). We have constructed these spectra following the trends observed previously for the dependence of photoionization cross sections on $\Delta N^+ = N^+ - N'$ changes. As shown in Figs. 4(a)–4(d), the good agreement observed between the simulated and experimental spectra can be taken as a support for the rotational assignments of the PFI-PE spectra. The least-squares fit to all the observed positions of the rotational transition peaks in these PFI-PE spectra based on the transition formula similar to Eq. (1) gives the rotational constant $B_0^+ = 0.7163 \pm 0.0021$ cm^{-1} and band origin $\nu_{00}^+ = 62\,383.05 \pm 0.14$ cm^{-1} for $CoC^+((X^1\Sigma^+; v^+ = 0)$. As pointed out above, the effective pulsed PFI field used is F = 0.4 V/cm. According to the Stark shift formula of $4(F)^{1/2}$ cm^{-1} for using a PFI field, the full width of the Stark shift is predicted to be 2.4 cm^{-1}.[20,21] We have shown previously that the peak of the PFI-PE band is shifted by 1.2 cm^{-1} (about one half of the full-width).[22] After taking into account this stark shift correction of 1.2 cm^{-1}, the adiabatic IE(CoC) is determined to be 62 384.3 ± 0.6 cm^{-1} (7.73467 ± 0.00007 eV).

The rotational selected and resolved PFI-PE spectra in the total $\omega_1 + \omega_2$ energy range of 63 300–63 402 cm^{-1} for the formation of CoC^+ $(X^1\Sigma^+; v^+ = 1; N^+)$ recorded by setting the VIS ω_1 energy to the rotational transitions, P(7), P(8), P(9), and P(10) of the excitation spectrum of Fig. 1 to selected $N' = 6$–9 rotational levels of the intermediate $CoC^*(^2\Sigma^+; v')$ state are depicted as the lower spectra in Figs. 5(a)–5(d), respectively. The corresponding UV ω_2 energy scanning range for the PFI-PE spectra of Figs. 5(a)–5(d) is 42 920–43 020 cm^{-1}. Similar to the PFI-PE spectra shown in Figs. 4(a)–4(d), we have identified three very strong background electron peaks (marked by asterisks) in the PFI-PE spectra for CoC^+ $(X^1\Sigma^+; v^+ = 1; N^+)$ of Figs. 5(a)–5(d). The upper spectra are the corresponding simulated spectra obtained by using a Gaussian instrumental line profile (FWHM of 1.5 cm^{-1}) for the PFI-PE resolution. On the basis of a least-square fit to the observed rotational transition peak positions, we have assigned the rotational transitions as marked on top of the simulation spectra. The rotational constant and band origin of the $CoC^+(X^1\Sigma^+; v^+ = 1)$ state were determined to be $B_1^+ = 0.7121 \pm 0.0018$ cm^{-1} and $\nu_{10}^+ = 63{,}357.4 \pm 0.6$ cm^{-1} (7.85532 ± 0.00007 eV) after taking into account the Stark shift correction.

Since most of the photoionization transitions from the $N' = 6$–9 levels of $CoC^*(^2\Sigma^+; v')$ to individual N^+ levels of CoC^+ $(X\ ^1\Sigma^+; v^+ = 0$ and 1) are well resolved

Downloaded 07 Mar 2013 to 18.85.28.26. Redistribution subject to AIP license or copyright; see http://jcp.aip.org/about/rights_and_permissions

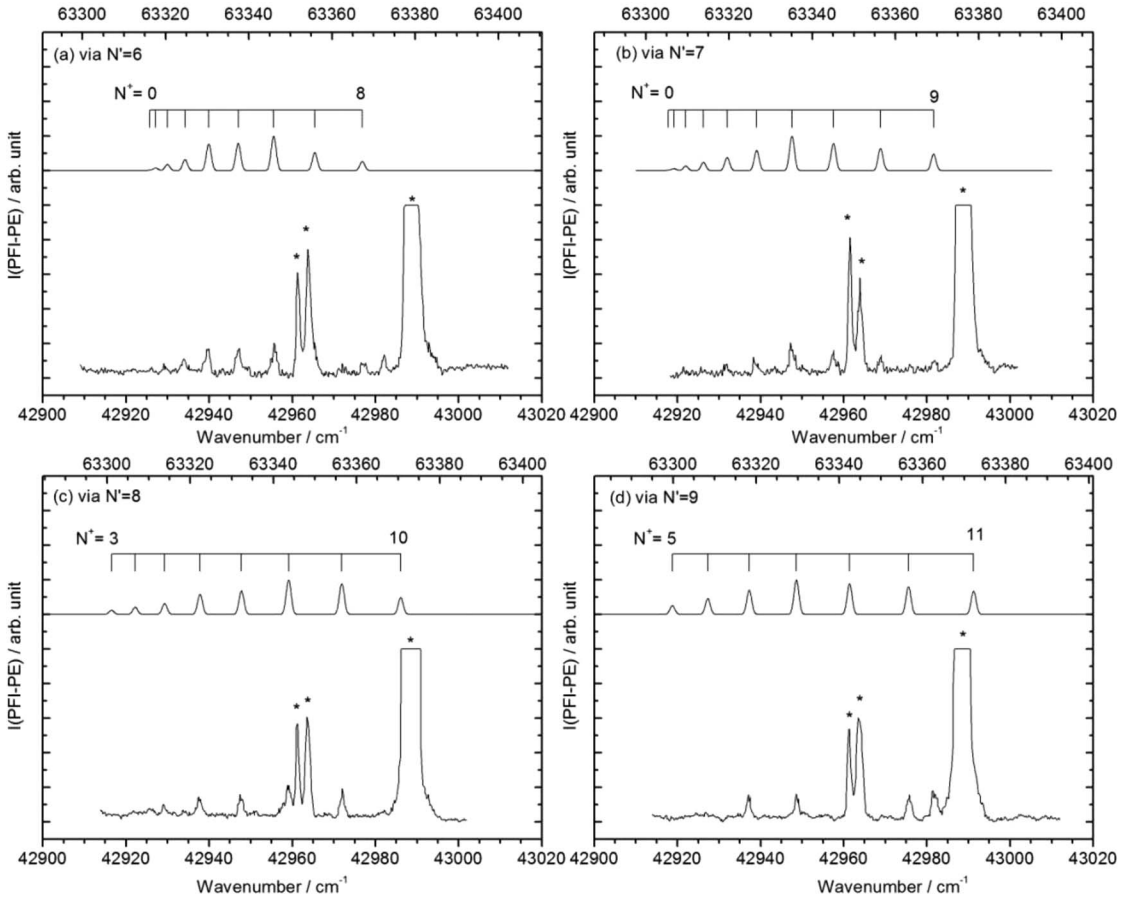

FIG. 5. Rotationally selected and resolved PFI-PE spectra (lower spectra) in the total $\omega_1 + \omega_2$ energy region of 63 300–63 402 cm^{-1} (top energy scale) for the formation of $CoC^+(X^1\Sigma^+; v^+ = 1; N^+)$ from the rotational levels, (a) $N' = 6$, (b) $N' = 7$, (c) $N' = 8$, and (d) $N' = 9$, of the $CoC^*(^2\Sigma^+; v')$ state. The corresponding UV ω_2 energies are in the range of 42 910–43 010 cm^{-1} (bottom energy scale). These N' levels were prepared by setting the VIS ω_1 energies at the respective P(7), P(8), P(9), and P(10) transition positions as marked in the excitation spectrum of Fig. 1. The individual simulated spectra obtained by using a Gaussian instrumental line profile (FWHM = 1.5 cm^{-1}) for the PFI-PE energy resolution profile are shown as the upper curves in (a)–(d). The peaks marked by asterisks are background electron peaks originated from electrons produced by one-color UV-UV resonance-enhanced photoionization of Co atoms.

and can clearly be identified in the PFI-PE spectra of Figs. 4(a)–4(d) and 5(a)–5(d) except at the energy regions near the Co atom resonance lines, it is interesting to examine the $\Delta N^+ = N^+ - N'$ changes observed in the photoionization transitions CoC^+ $(X\ ^1\Sigma^+; v^+ = 0$ and 1; $N^+) \leftarrow CoC^*(^2\Sigma^+; v'; N')$. As expected, the most intense ΔN^+ transition observed from a given N' level is the $\Delta N^+ = 0$ transition, corresponding to the smallest change in core rotational angular momentum. However, previous studies have shown that photoionization transitions with large ΔN^+ changes can be facilitated by rotational autoionization. The intensity for the $|\Delta N^+|$ transition is found to decrease as $|\Delta N^+|$ is increased. This observation is consistent with the ΔN^+ changes observed in the state-to-state photoionization studies of CH_3I, CH_3Br, FeC, and NiC.[10,11,23–25] Due to the interference of the background electron peaks, the maximum ΔN^+ change observed in the PFI-PE spectra of Figs. 4(a)–4(d) for the CoC^+ $(X\ ^1\Sigma^+; v^+ = 0)$ is limited to 3 or 4 and the lowest rotational level identified is $N^+ = 2$ from $N' = 6$. Since the interference by the background electron peaks is less severe in the PFI-PE spectra for the CoC^+ $(X^1\Sigma^+; v^+ = 1)$ shown in Figs. 5(a)–5(d), the maximum change in rotational angular momentum is observed to be $\Delta N^+ = 6$ from $N' = 6$. The latter transition corresponds to the formation of CoC^+ $(X^1\Sigma^+; v^+ = 0; N^+ = 0)$ as marked in Fig. 5(a); and thus confirming that the ground state of CoC^+ is of $^1\Sigma^+$ symmetry.

The PFI-PE signal for the formation of $CoC^+(X^1\Sigma^+; v^+ = 2; N^+)$ was too weak for single rovibronically selected measurements to be made. The PFI-PE spectrum for CoC^+ $(X^1\Sigma^+; v^+ = 2; N^+)$ (top black spectrum of Fig. 6) with acceptable signal-to-noise ratios could only be obtained by setting the VIS ω_1 energy at 20 408.5 cm^{-1} of the excitation spectrum of Fig. 1. The PFI-PE spectrum thus obtained for $CoC^+(X^1\Sigma^+; v^+ = 2; N^+)$ has contributions from the $CoC^*(^2\Sigma^+; v'; N' = 4–8)$ states. The simulated N'-selected PFI-PE spectra for $N' = 4–8$ are depicted as the red, green, orange, purple, and pink spectra in Fig. 6. The relative intensities of these simulated N'-selected PFI-PE spectra have been scaled to be consistent with the estimated populations of the rotational levels $N' = 4–8$ based on the Boltzmann distribution as well as the offsets in the excitation of these rotational states. We find that in order to obtain a better fit to the experimental PFI-PE spectrum for the $v^+ = 2$ vibrational band, the intensities of the positive ΔN^+ branches for these N'-selected PFI-PE spectra have to be suppressed relative to those of the corresponding

Downloaded 07 Mar 2013 to 18.85.28.26. Redistribution subject to AIP license or copyright; see http://jcp.aip.org/about/rights_and_permissions

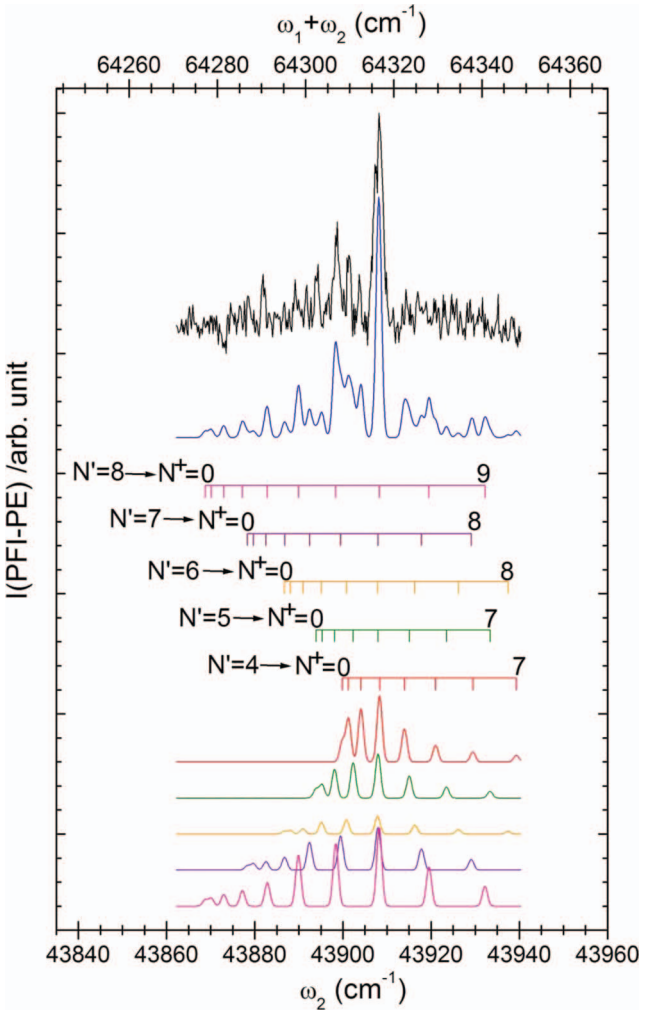

FIG. 6. The PFI-PE spectra (top spectrum) for the formation of $CoC^+(X^1\Sigma^+; v^+ = 2; N^+)$ recorded by setting the VIS ω_1 energy at the band head (20 408.5 cm^{-1}) of the excitation spectrum of Fig. 1, while scanning UV photon ω_2 in the range of 43 862–43 940 cm^{-1}. Based on the spectral simulation, the rotational levels $N' = 4$-8 are expected to contribute to the PFI-PE measurements. The (blue) spectrum shown below the PFI-PE spectrum is the best simulated spectrum obtained by summing the individual simulated spectra from the $N' = 4$-8 levels of the intermediate $CoC^*(^2\Sigma^+; v')$ state. The individual simulated spectra were obtained by assuming a Gaussian instrumental line profile (FWHM = 1.5 cm^{-1}) for the PFI-PE energy resolution profile.

negative ΔN^+ branches. Due to the forced rotational autoionization mechanism,[23–26] the higher intensities for the negative ΔN^+ branches are to be expected. The observation of large negative ΔN^+ changes was also reported by Harrington and Weisshaar[27] in the two-color resonance-enhanced PFI-PE study of the VO/VO^+ system. In order to rationalize this observation, they have invoked a breakdown of case (d) coupling to explain oscillator strength in the field of the large dipole moment associated with VO. The best simulated spectrum (blue spectrum of Fig. 6) obtained by summing up all these N'-selected PFI-PE spectra are in reasonable good agreement with the experimental PFI-PE spectrum. The simulation has provided the rotational constant $B_2^+ = 0.705 \pm 0.0050$ cm^{-1} and the band origin $\nu_{20}^+ = 64\,317.6 \pm 0.6$ cm^{-1} for the $CoC^+(X^1\Sigma^+; v^+ = 2)$ vibrational band after taking into account the Stark shift correction.

The IE(CoC) = 62 384.3 ± 0.6 cm^{-1} (7.73467 ± 0.00007 eV) determined in this study, along with the IE(Co) = 63 564.6 ± 1.0 cm^{-1} (7.88101 ± 0.00012 eV) reported previously by Page and Gudeman[28] has allowed the determination of the difference between the IE(Co) and IE(CoC) to be 0.14630 ± 0.00014 eV. On the basis of the conservation of energy, the latter value is equal to D_0 (Co^+−C) − D_0 (Co−C). As pointed out above, the main electronic configuration of the $CoC(X^2\Sigma^+)$ ground states is $\ldots 7\sigma^2\ 8\sigma^2\ 3\pi^4\ 1\delta^4\ 9\sigma^1$. The formation of the $CoC^+(X^1\Sigma^+)$ ground state with the main electronic configuration of $\ldots 7\sigma^2\ 8\sigma^2\ 3\pi^4\ 1\delta^4$ involves the removal of the electron residing in the highest occupied 9σ molecular orbital, the small difference observed between the Co–C^+ and Co–C bonds indicates that the 9σ molecular orbital is mostly nonbonding in nature.

Based on the least squared fit to the experimental rotational constants B_0^+, B_1^+, and B_2^+ to the standard formula

$$B_v^+ = B_e^+ - \alpha_e^+(v^+ + 1/2), \tag{2}$$

we have obtained the rotational constants $B_e^+ = 0.7196 \pm 0.0005$ cm^{-1} and $\alpha_e^+ = 0.0056 \pm 0.0008$ cm^{-1}. The B_e^+ value has enabled the determination of the equilibrium bond distance $r_e^+ = 1.534$ Å for the $CoC^+(X^1\Sigma^+)$ ground state.

The expression for the spacing between two adjacent vibrational levels can be written as $\Delta G(v^+ + 1/2) = G(v^+ + 1)$

TABLE I. Energetic and spectroscopic data obtained in the present PIE and PFI-PE study, including ionization energies (IEs) for the formation of $CoC^+(X^1\Sigma^+; v^+ = 0$–$2)$, rotational constants ($B_0^+$, B_1^+, B_2^+, B_e^+, and α_e^+), equilibrium bond distance (r_e^+), and vibrational constants ($\Delta G(1/2)$, $\Delta G(3/2)$, ω_e^+, and $\omega_e^+\chi_e^+$) for $CoC^+(X^1\Sigma^+; v^+ = 0$–$2)$, and the difference of D_0 values for $CoC^+(X^1\Sigma^+)$ and $CoC(X^2\Sigma^+)$.

$CoC^+(X^1\Sigma^+; v^+)$	This work
$v^+ = 0$	
ν_{00}^+ (cm^{-1})	62 384.3 ± 0.6[a]
IE (cm^{-1})	62 384.3 ± 0.6[a] 62 381 ± 6[b]
B_0^+ (cm^{-1})	0.7163 ± 0.0021
$v^+ = 1$	
ν_{10}^+ (cm^{-1})	63 357.4 ± 0.6[a]
IE (cm^{-1})	63 357.4 ± 0.6[a] 63 363 ± 6[b]
B_1^+ (cm^{-1})	0.7121 ± 0.0018
$v^+ = 2$	
ν_{20}^+ (cm^{-1})	64 317.6 ± 0.6[a]
IE (cm^{-1})	64 317.6 ± 0.6[a] 64 301 ± 6[b]
B_2^+ (cm^{-1})	0.7050 ± 0.0050
Rotational constants	
B_e^+ (cm^{-1})	0.7196 ± 0.0005
α_e^+ (cm^{-1})	0.0056 ± 0.0008
r_e^+ (Å)	1.534
Vibrational constants	
$\Delta G(1/2)$ (cm^{-1})	973.1 ± 0.6
$\Delta G(3/2)$ (cm^{-1})	960.6 ± 0.6
ω_e^+(cm^{-1})	985.6 ± 0.6
$\omega_e^+\chi_e^+$ (cm^{-1})	6.3 ± 0.6
Bond dissociation energies	
D_0 (Co^+−C) - D_0 (Co−C) (eV)	0.14630 ± 0.00014

[a]This work. Based on PFI-PE measurements.
[b]This work. Based on PIE measurements.

Downloaded 07 Mar 2013 to 18.85.28.26. Redistribution subject to AIP license or copyright; see http://jcp.aip.org/about/rights_and_permissions

$-$ G(v^+), where G(v^+) = $\omega_e{}^+(v^+{+}1/2) - \omega_e{}^+\chi_e{}^+(v^+{+}1/2)^2$. Based on the PFI-PE measurement, we have determined $\Delta G(1/2) = 973.1 \pm 0.6$ cm^{-1} and $\Delta G(3/2) = 960.6 \pm 0.6$ cm^{-1}. These values in turn allow the determination of $\omega_e{}^+ = 985.6 \pm 0.6$ cm^{-1} and $\omega_e{}^+\chi_e{}^+ = 6.3 \pm 0.6$ cm^{-1}. All spectroscopic constants associated with $CoC^+(X^1\Sigma^+; v^+ = 0–2)$ determined by the PIE and PFI-PE measurements are listed in Table I. Their comparison with the CCSDTQ(Full) predictions is the main theme of the companion theoretical article.

IV. CONCLUSIONS

We have performed a two-color VIS-UV resonance-enhanced PIE and PFI-PE study on cold gaseous $CoC(X^2\Sigma^+; v'' = 0)$ prepared by a laser ablation supersonically cooled beam source. This rotationally selected and resolved PFI-PE study has shown that the CoC^+ ground state is of $^1\Sigma^+$ symmetry. Furthermore, the unambiguous rotational assignment of the PFI-PE spectra for the formation of $CoC^+(X^1\Sigma^+; v^+ = 0–2, N^+)$ has allowed the determination of highly precise values for the IE(CoC), vibrational and rotational constants for $CoC^+(X^1\Sigma^+; v^+ = 0–2)$, and the difference in 0 K bond energies between the CoC^+ cation and the CoC neutral. The detailed comparison of the energetic and spectroscopic data determined in the present study with predictions of state-of-the-art *ab initio* quantum calculations are presented in the companion[17] article. This high-resolution PFI-PE study along with the previous studies of the FeC/FeC$^+$ and NiC/NiC$^+$ systems has provided a sufficiently large database for serving as a reliable benchmark for testing the reliability of predictions based on state-of-the-art quantum theoretical package, such as the CCSDTQ/CBS procedures. On the basis of the comparisons between the experimental and theoretical results,[17] we conclude that the CCSDTQ/CBS approach is capable of providing reliable energetic predictions, such as IEs and D_0s for 3*d*-transition metal carbides and their cations in their ground states, with errors of 40–50 meV.

ACKNOWLEDGMENTS

This work was supported by the National Science Foundation (NSF) Chemical Structures, Dynamics, and Mechanisms Program Grant No. CHE 0910488. The VUV laser system used was constructed by the NSF Chemical Instrumentation Program Grant No. CHE 0342829. The construction of the photoion-photoelectron apparatus used in this study was partially financed by the U.S. Department of Energy-Basic Energy Sciences (DE-FG02-02ER15306).

[1] Landolt-Börnstein, *Astronomy and Astrophysics*, New Series Group 6 Vol. 1 (Spring-Verlag, Berlin, 1965).
[2] J. F. Harrison, Chem. Rev. **100**, 679–716 (2000).
[3] M. A. Brewster and L. M. Ziury, Astrophys. J. **559**, L163 (2001).
[4] A. J. Merer, Annu. Rev. Phys. Chem. **40**, 407 (1989) and references therein.
[5] J. M. Thomas, B. F. G. Johnson, R. Raja, G. Sankar, and P. A. Midgley, Acc. Chem. Res. **36**, 20 (2003).
[6] R. J. Van Zee, J. J. Bianchini, and W. Weltner, Jr., Chem. Phys. Lett. **127**, 314 (1986).
[7] A. G. Adam and J. R. D. Peers, J. Mol. Spectrosc. **181**, 24 (1997).
[8] M. Barnes, A. J. Merer, and G. F. Metha, J. Chem. Phys. **103**, 8360 (1995).
[9] J. R. Guo, Z. X. Zhang, T. T. Wang, C. X. Chen, and Y. Chen, Chin. J. Chem. Phys. **21**, 505 (2008).
[10] Y. C. Chang, C. S. Lam, B. Reed, K. C. Lau, H. T. Liou, and C. Y. Ng, J. Phys. Chem. A **113**, 4242 (2009).
[11] Y. C. Chang, X. Shi, K. C. Lau, Q. Z. Yin, H. T. Liou, and C. Y. Ng, J. Chem. Phys. **133**, 054310 (2010).
[12] A. C. Borin, J. P. Gobbo, and B. O. Roos, Chem. Phys. Lett. **418**, 311 (2006).
[13] G. L. Gutsev, L. Andrews, and C. W. Bauschlicher, Jr., Theor. Chem. Acc. **109**, 298 (2003).
[14] D. Tzeli and A. Mavridis, J. Phys. Chem. A **110**, 8952 (2006).
[15] K. C. Lau, Y. C. Chang, C. S. Lam, and C. Y. Ng, J. Phys. Chem. A **113**, 14321 (2009).
[16] K. C. Lau, Y. C. Chang, X. Shi, and C. Y. Ng, J. Chem. Phys. **133**, 114304 (2010).
[17] K.-C. Lau, Y. Pan, C.-S. Lam, H. Huang, Y.-C. Chang, Z. Luo, X. Shi, and C. Y. Ng, J. Chem. Phys. **138**, 094302 (2013).
[18] T. G. Dietz, M. A. Duncan, D. E. Powers, and R. E. smalley, J. Chem. Phys. **74**, 6511 (1981).
[19] Y. C. Chang, H. Xu, Y.-T. Xu, Z. Lu, Y.-H. Chiu, D. J. Levandier, and C. Y. Ng, J. Chem. Phys. **134**, 201105 (2011).
[20] W. A. Chupka, J. Chem. Phys. **98**, 4520 (1993).
[21] C. Y. Ng, Annu. Rev. Phys. Chem. **53**, 101 (2002).
[22] H. Gao, Y.-T. Xu, L. Yang, C.-S. Lam, H.-L. Wang, J.-G. Zhou, and C. Y. Ng, J. Chem. Phys. **135**, 224304 (2011).
[23] X. Xing, B. Reed, M.-K. Bahng, S. J. Baek, P. Wang, and C. Y. Ng, J. Chem. Phys. **128**, 104306 (2008).
[24] P. Wang, X. Xing, K.-C. Lau, H. K. Woo, and C. Y. Ng, J. Chem. Phys. **121**, 7049 (2004).
[25] X. Xing, P. Wang, B. Reed, S. J. Baek, and C. Y. Ng, J. Phys. Chem. A **112**, 9277 (2008).
[26] Y. Emily, H. Hanspeter, and K. Ravinder, Phys. Rev. A **38**, 1666 (1988).
[27] J. Harrington and J. C. Weisshaar, J. Chem. Phys. **97**, 2809 (1992).
[28] R. H. Page and C. S. Gudeman, J. Opt. Soc. Am. B **7**, 1761 (1990).

Downloaded 07 Mar 2013 to 18.85.28.26. Redistribution subject to AIP license or copyright; see http://jcp.aip.org/about/rights_and_permissions